Journal of Engineering Issues and Solutions

Vulnerability assessment of touristic village in Nepal Himalayas: A case study of Lwang village

Pradeep Kafle[1], Magnus Upadhyay[1], Shreedhar Khakurel[1,*]

[1] *Department of Civil Engineering, Pashchimanchal Campus, Institute of Engineering, Pokhara, Nepal*

**Corresponding email: shreedhar.khakurel@ioepas.edu.np*

Received: June 21, 2024; Revised: July 5, 2024; Accepted: July 6, 2024

doi: https://doi.org/10.3126/joeis.v3i1.67094

Abstract

Nepal is located in a seismically active zone and masonry structures are widely constructed throughout the country. Lwang village, a popular tourist destination in Western Nepal, contains several masonry houses. This study aims to assess the seismic vulnerability of these buildings using a vulnerability index (*Iv*) method. Vulnerability curves were developed for all the studied 24 houses resulting in a mean *Iv* of 71.3. From these vulnerability curves, the expected damage grades for each building for the 2023 Jajarkot (Intensity VII) and 2015 Gorkha (Intensity X) earthquakes were determined as per EMS-98. Results showed that during an earthquake of intensity comparable to the Jajarkot event, a significant proportion of buildings would experience moderate to heavy damage. Furthermore, an earthquake similar to the Gorkha event would result in very heavy damage to near collapse for many structures. Specifically, 45.83 % of the buildings are expected to suffer heavy damage, and 50 % could face near-collapse during an earthquake event of Intensity X (MMI Scale). These findings highlight the urgent need for targeted strengthening measures to enhance the seismic resilience of buildings in Lwang Village, thereby safeguarding both the local community and the area's touristic value.

Keywords: *Building damage, earthquake, masonry house, vulnerability curve, vulnerability index*

1. Introduction

The Himalayas, formed by the collision of the northward-moving Indian continent with the Asian landmasses, include Nepal at their central sector covering 800 km of the 2800 km - long range, and uniquely expose a cross-section over 40 km thick from roots to peaks in a single traverse (Upreti, 1999). The plate movement is an ongoing geological process, occurring at a displacement rate of about two centimetre per year, periodically releasing accumulated stress, and causing earthquakes (Bettinelli et al., 2006). In the recent past, Nepal has experienced devastating earthquakes, such as the 2015 Gorkha earthquake with a moment magnitude 7.8 and the 2023 Jajarkot earthquake with a moment magnitude 5.7. Unreinforced masonry (URM) has been the predominant material used for constructing buildings in the Nepal Himalayas from the beginning of

civilisation. These structures are built with or without mud mortar, depending on the particular region of the Himalayas (Khadka, 2020). Given economic constraints, stone masonry replacement is unfeasible in rural Nepal, alarming urgent implementation of seismic safety measures at life-preserving levels, especially as 38% of the entire building inventory experienced Damage State 5 (EMS-98) in the 2015 Gorkha earthquake (Gautam, 2018). Damageability functions of masonry buildings in different regions of Nepal also showed those structures to be fragile under seismic action (Gautam et al., 2021).

The vulnerability curve is one of the important parameters for post-earthquake building assessments (Khakurel et. al., 2023). Understanding the vulnerability of masonry structures in Lwang village in the Kaski district subjected to seismic forces is crucial due to their architectural importance, cultural heritage value, and susceptibility to earthquake-induced damage. Factors such as inadequate lateral load resistance, weak mortar, lack of reinforcement, and deteriorating materials result in the vulnerability of the prevalent masonry buildings in the village to lateral forces. The seismic threat to Lwang village raises significant concerns about the structural stability and preservation of its buildings.

This study assesses the seismic vulnerability of masonry structures commonly built in the Mid-Himalayan region of Nepal, particularly from Lwang village. Furthermore, damage grades of the buildings in the region are predicted based on the intensities of the past earthquakes. The insights gained from the Lwang village study can be applied to other regions with similar building typologies, thereby helping to mitigate vulnerability.

2. Materials and Methods

2.1 Building description

Machhapuchchhre Rural Municipality is situated in the mid-Himalayan region of Nepal which is prone to frequent earthquakes. The study area, Lwang village, is situated in the Machhapuchchhre Rural Municipality, ward number 8, approximately 25 km northwest of Pokhara. Positioned at a latitude of 83.9003 °*E* and longitude of 28.4317 °*N*, with an elevation of 1550 m, the village is renowned for its natural beauty and cultural significance, making it a popular tourist destination. As per the National Housing Population Census (NHPC, 2021), 55.3% of buildings make use of mud-bonded bricks/stone in this area and 42.7% of them employ cement-bonded bricks/stone material in their outer walls. The location map of the study area is shown in the Figure 1.

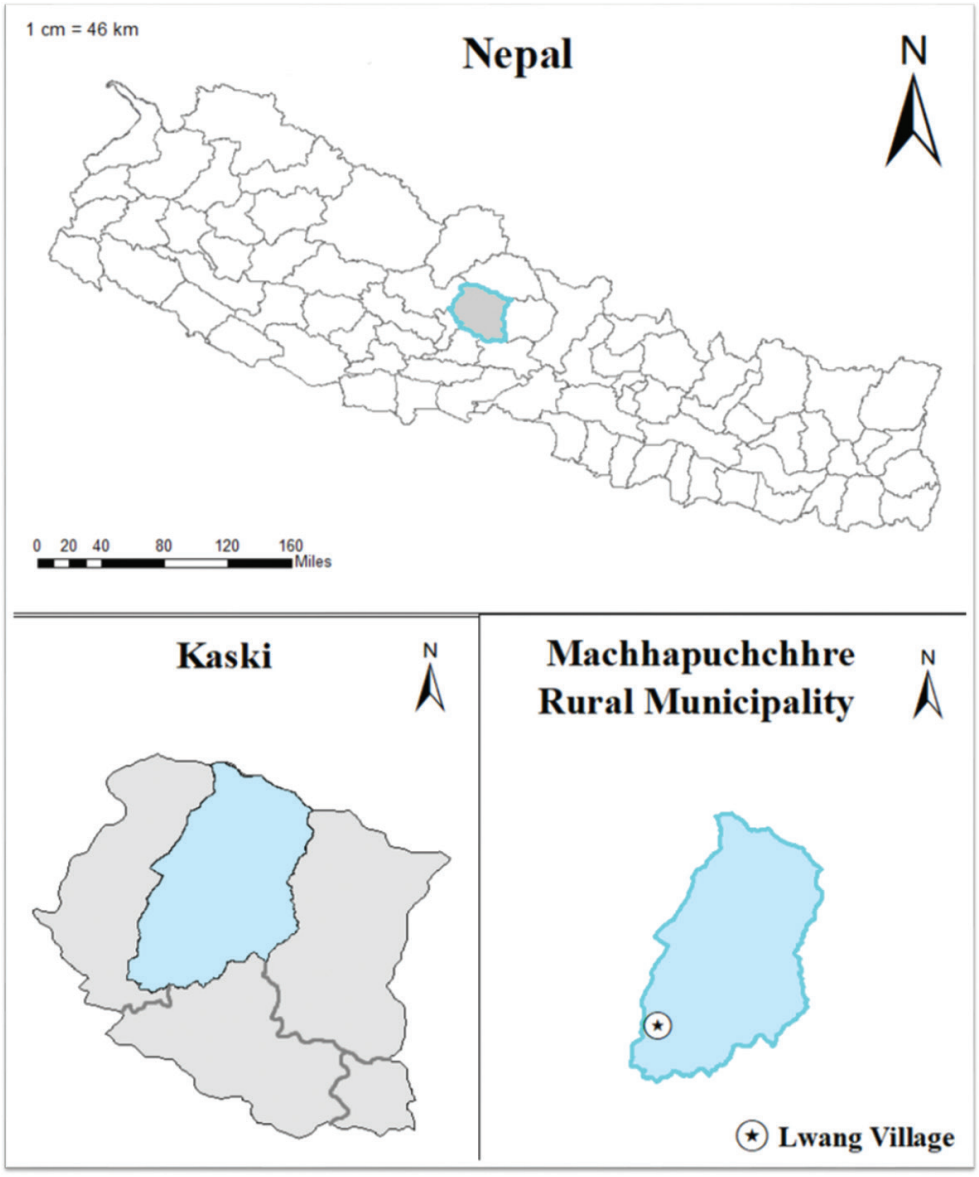

Figure 1: Location map of study area

The village as shown in Figure 2 is distinguished by its prevalent use of stone masonry construction presenting distinct challenges regarding seismic vulnerability due to the material characteristics and construction methods adopted. Stone masonry constitutes stone as a unit and mud or cement or both as mortar. Due to the presence of these brittle materials and the absence or minimal presence of additional ductile members, they are susceptible to lateral loadings including earthquakes.

Figure 2: Lwang village with stone masonry houses

The flowchart of the methodology proposed for this study is presented in Figure 3. The study is initiated from data collection by field visit and literature review. Then, the vulnerability index is calculated from the building parameters, vulnerability class values, and weightage of the parameters. In doing so, parameters are chosen based on past studies to calculate the vulnerability score. From the computed vulnerability index, a vulnerability curve is produced which helps to predict the damage grade of buildings at earthquakes of different intensities.

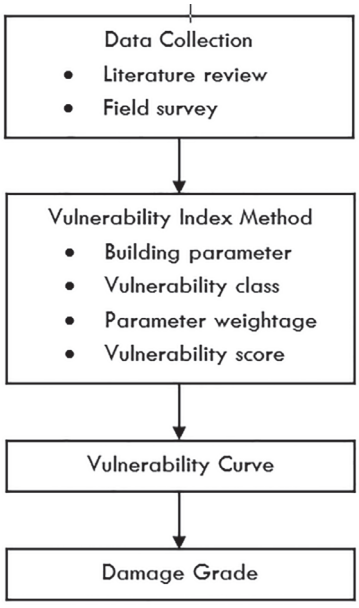

Figure 3: Flowchart of the study methodology

2.2 Data collection

Field survey is conducted in Lwang village to identify the buildings for the study. 24 buildings were studied consisting mostly of stone masonry structures and a few brick masonry structures as shown in Figure 4. Most of these buildings use mud mortar while a few use cement mortar. The study considered various parameters including building usage, number of storeys, type of mortar, type of stone, type of roof, seismic resistance elements, plan area, and crack patterns. Additionally, verbal conversations with homeowners provided details about the foundations and the construction years of the buildings. Field observations and conversations revealed that the majority of buildings were constructed as non-engineered structures. However, there has been a shift from non-engineered construction to pre-engineered and engineered housing construction post-2015.

Figure 4. Photos of the studied buildings

2.3 Vulnerability index method

Numerous factors come into play, including the dimensions and mechanical properties of the units, the thickness and mechanical characteristics of the mortar, unit laying patterns, and workmanship. These factors collectively influence the performance of masonry when subjected to vertical or horizontal loads (Lourenco, 1996). Vulnerability index methods require the definition of (a) various parameters that represent the characteristics of vernacular buildings affecting their seismic performance; (b) seismic vulnerability classes assigned to each parameter; and (c) weights assigned to each parameter. Based on the available information, Dolce et al. (1994) classified methodologies of index method as empirical, analytical, experimental, and hybrid. In this study, the empirical approach is employed which was first presented in GNDT-SSN-1994 and improved later by Ortega et al. (2019). Among other empirical approaches, this approach is hybrid as it relates vulnerability score with damage grade (based on EMS-98) and intensity of the earthquake (MMI scale). This method, which merges the seismic vulnerability index formulation with the macro seismic approach, has recently been applied to assess the seismic vulnerability of masonry structures in numerous historic city centres (Neves et al., 2012; Ferreira et al., 2013; Ferreira et al., 2017).

This particular approach is adopted to assess the seismic vulnerability of various Nepali temples (Shakya et al., 2014, Upadhyay et al., 2024). A similar strategy was also adopted in assessing the vulnerability of Nepali school buildings under seismic action after 2015 Gorkha earthquake (Gautam et al., 2020). These different studies adopted parameters with slight differences in weightage based on their area of study. Shakya et al. (2014) included additional parameters: soil conditions at the site and irregularities in their assessments. Similarly, Gautam et al. (2020) accounted for workmanship and age factors which include material deterioration. Although these factors are not explicitly included in this study, they are attempted to address through the state of conservation (P9) parameter. Gautam et al. (2020) also considered seismic components such as bands and seismic enhancements, as well as retrofitting and structural pounding. Moreover, parameter regarding the type of foundations is not incorporated in this study although all studied buildings possess similar strip wall footings. None of the studied buildings had retrofitting, stitches, or other seismic enhancers.

In this study, ten parameters and their respective weightages are adopted as proposed by Ortega et al. (2019) which are discussed in detail hereunder.

1. Wall slenderness (P1): The out-of-plane behaviour of walls is greatly influenced by their slenderness, and this parameter has been utilized by many researchers to evaluate the seismic vulnerability of masonry walls (Spence & D'Ayala, 1999; Lourenco et al., 2013). The slenderness of these walls determined from the ratio of effective height/length and thickness assign building classes i.e., class A ($\lambda \leq 6$), class B ($6 < \lambda \leq 9$), class C ($9 < \lambda \leq 12$), and class D ($\lambda > 12$) (Ortega et al., 2019).
2. Maximum wall span (P2): The maximum wall span is another geometric factor that influences the out-of-plane response of walls. Formulations of vulnerability indexes incorporating this factor suggest a classification based on the ratio of span to thickness (Vicente et al., 2011). Considering that wall thickness is already accounted for in the first parameter, this factor solely examines the variation in the maximum wall span which classify buildings into class A (Smax < 5), class B ($5 \leq$ Smax < 7), class C ($7 \leq$ Smax < 9), and class D (Smax $\geq$ 9) (Ortega et al., 2019).
3. Type of material (P3): Masonry constructions often utilize materials like rammed earth, stone, adobe, and fired clay brick, each contributing to a range of structural typologies and wall morphologies (Ortega et al., 2019). The variations in masonry include:
    a) Various types, sizes, and shapes of masonry units are used, including fired clay brick masonry, ashlar stone masonry, and irregular rubble stone masonry.

b) Variations in masonry layout encompass irregular or regular horizontal courses, the inclusion of multiple leaves, and the lack of connections between these leaves.

c) The use of various types of mortar, when applied, also plays a crucial role. These factors collectively determine the quality of the masonry, thereby influencing the building's seismic resilience.

4. Wall-to-wall connection (P4): To assess the impact of this parameter directly, the mechanical strength of the corner elements is intentionally reduced to mimic weak connections. These weaker connections are more prone to failure, leading to the independent behaviour of perpendicular walls. This method of simulating weak connections in rammed-earth buildings underscores the difficulties in forming corners within the frameworks and the inadequacies of vertical recess joint solutions (Angulo-Ibanez et al., 2012). In stone masonry buildings, this signifies the existence of vertical joints, thereby indicating a deficiency in proper interlocking between orthogonal walls (Ortega et al., 2019).
5. Horizontal diaphragms (P5): Horizontal timber diaphragms play a pivotal role in directing lateral earthquake forces toward the vertical resistance components of the structure. The pliability of traditional timber floors in unreinforced masonry and earthen vernacular buildings results in notable bending and shear distortions when subjected to horizontal loads (Mendes & Lourenco, 2015). The seismic response of vernacular buildings heavily relies on the characteristics of timber diaphragms, where proper connections and sufficient in-plane stiffness mitigate local out-of-plane failures of load-bearing walls during earthquake loading (Ortega et al., 2018).
6. Roof thrust (P6): The presence or absence of lateral thrust from roofing structural systems significantly influences the out-of-plane collapse mechanism of load-bearing walls. Roof types that exert lateral thrust, such as those with unconnected rafters, can push supporting walls outward under vertical loads, underscoring the pivotal role of roof type in the seismic behaviour of buildings (Ortega et al., 2019).
7. Wall openings (P7): Openings in earthquake-resistant walls diminish their resistance to in-plane forces, especially in buildings susceptible to such damage. Adequately connected diaphragms can avert premature collapses. Post-earthquake damage frequently reflects the distribution of facade openings, accentuating their vulnerability. Based on wall openings, buildings are classified into different classes i.e., class A (IP < 10 %), class B (10 % $\leq$ IP < 25 %), class C (25 % $\leq$ IP < 40 %), and class D (IP$\geq$40 %) (Ortega et al., 2019).
8. Number of floors (P8): Taller buildings are more earthquake-prone due to their higher centre of gravity, resulting in increased wall overturning moments from horizontal loading. Different building classes are assigned based on the number of storeys such as class A (single storey), class B (one and half storey), class C (two storey), and class D (greater than two storey) (Ortega et al., 2019).
9. State of conservation (P9): The state of conservation is crucial for maintaining the stiffness and strength of masonry structures. Neglecting maintenance and repairs can greatly heighten the vulnerability of these structures (Masciotta et al., 2016).
10. In-plane index (P10): The in-plane index ratio estimates shear strength in orthogonal directions, serving as an indicator of the building's in-plane irregularity. It gauges the structure's stiffness in the main directions, reflecting its seismic performance potential (Lourenco et al., 2013). In-plane index assigns building as class A ($\gamma \geq 0.65$), class B ($0.55 \leq \gamma < 0.65$), class C ($0.45 \leq \gamma < 0.55$), and class D ($\gamma < 0.45$).

The vulnerability index formulation based on the Ortega et. al. (2019) from these ten parameters is presented in Table 1. Class A, which corresponds to the lowest vulnerability, has a qualification coefficient of ($C_{vi} = 0$). Conversely, Class D, representing the highest vulnerability, has a qualification coefficient of ($C_{vi} = 50$). Each parameter is assigned a weight (P_i) indicating its relative importance, ranging from 0.5 for the least important to 1.5 for the most important.

Table 1: Vulnerability index formulation (Ortega et al., 2019)

Symbol	Parameter	Class (C_{vi})				Weight (P_i)
		A	B	C	D	
P1	Wall slenderness	0	5	20	50	1
P2	Maximum wall span	0	5	20	50	0.5
P3	Type of material	0	5	20	50	1.5
P4	Wall-to-wall connections	0	5	20	50	0.75
P5	Horizontal diaphragms	0	5	20	50	1.5
P6	Roof thrust	0	5	20	50	0.5
P7	Wall openings	0	5	20	50	1.5
P8	Number of floors	0	5	20	50	1.5
P9	State of conservation	0	5	20	50	0.75
P10	In-plane index	0	5	20	50	0.5

The Vulnerability Index (I_v) is calculated using the qualification coefficient (C_{vi}) and weighted values of each parameter (P_i) as shown in Equation 1.

$$Vulnerability\ index\ (I_V) = \sum_{n=1}^{10} C_{vi}\ P_i \quad \text{.....(1)}$$

Moreover, the index value can be expressed in terms of normalized index $0 \leq I_v \leq 100$; higher value indicating more vulnerability. Further, this vulnerability index (I_v) can be expressed in terms of vulnerability index from macro seismic method (V) using Equation 2 (Da Silva Vicente, 2008),

$$V = 0.56 + 0.0064\ I_v \quad \text{.....(2)}$$

Finally, analytical expression from the macro seismic method as shown in Equation 3 can be used to estimate mean damage grade (μ_d) for different intensity levels of earthquakes (I), and the vulnerability curve can be plotted consequently.

$$\mu_d = 2.5 * \left(1 + \tanh\left(\frac{I + 6.25 * V - 13.1}{Q}\right)\right) \quad \text{.....(3)}$$

Here, I is earthquake intensity, V is the vulnerability index and Q is the ductility index, typically ranging from 1 to 4 (Vicente et al., 2011). It should be noted that the vulnerability indexes used by the two methods, I_v and V, differ from each other.

3. Results and Discussion

The data collected from the Lwang village is analysed and plotted in Figure 5. Based on the building usage, two-thirds of the buildings are residential (16), one-fourth are homestay, and the others are used for store, and public health. Three-fourths of the buildings (18) were constructed before the 2015 Gorkha earthquake while one-fourth of them were constructed after the earthquake. Based on the number of storeys, half of the buildings (12) are two-storey, 10 buildings are one and a half storey and the rest are single-storey. Among the studied 24 buildings, two-thirds of buildings (16) have slate roofs while one-third have metal sheets.

Based on the unit used, about four-fifths of the stone masonry buildings (19) have semi-coursed stone, 3 buildings use uncoursed stone, while the rest have coursed stone. Finally, five-sixths of the buildings used mud mortar while the rest buildings either used cement mortar or mixed one.

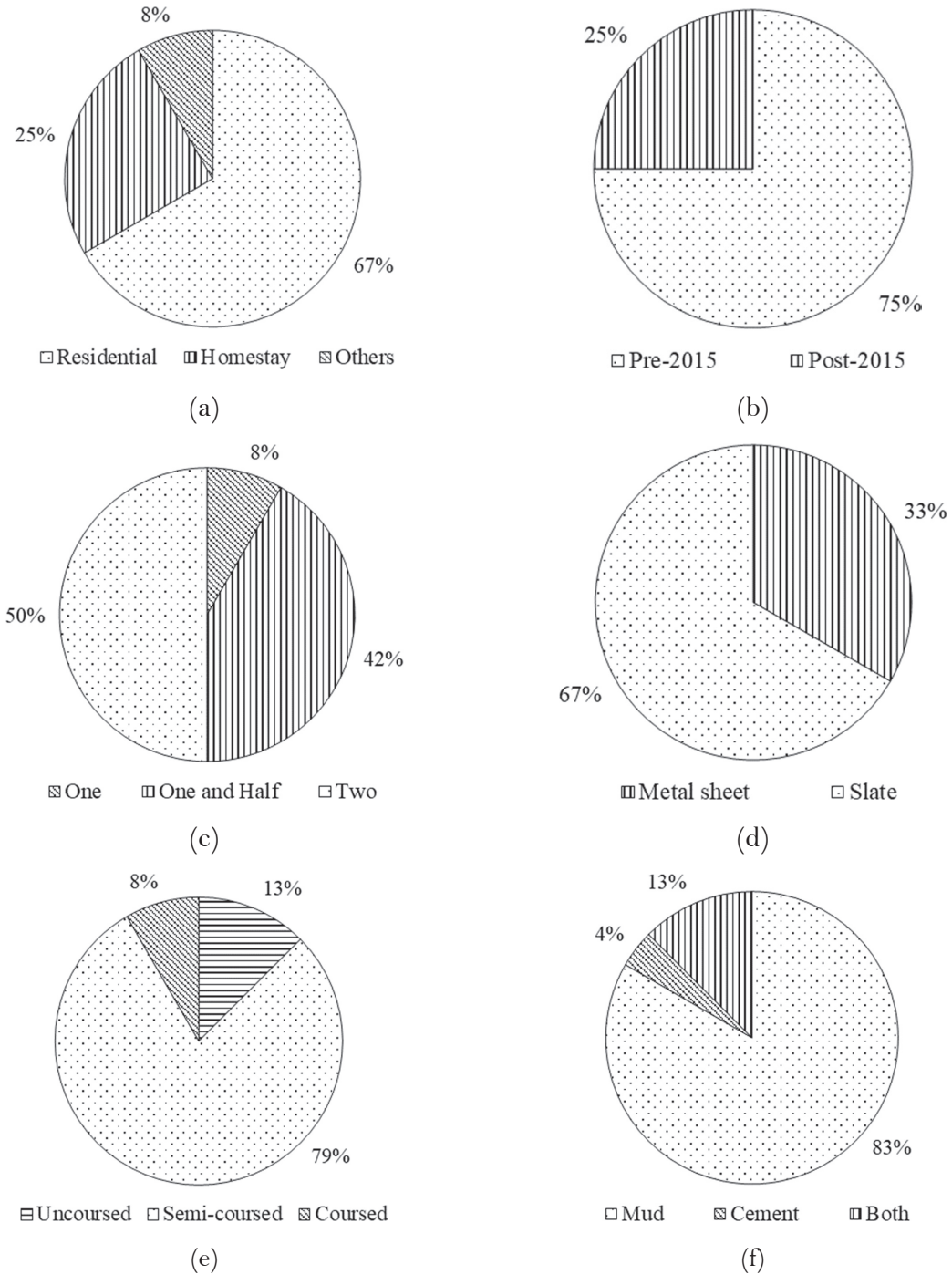

Figure 5: Percentage households based on (a) building usage, (b) built year w.r.t. the 2015 Gorkha earthquake, (c) number of storey, (d) type of roof, (e) type of stone, and (f) type of mortar

In Lwang village, the vulnerability assessment of masonry structures reveals distinct characteristics across ten parameters. The village predominantly features masonry walls with favourable slenderness ratios (100% in Class A), as shown in Table 2, reducing susceptibility to out-of-plane failure. Most walls exhibit moderate maximum spans relative to thickness (66.66% in Class A, 29.17% in Class B), promoting structural stability. Stone masonry with mud is prominently used (75% in Class B), enhancing resilience compared to other materials (eg. Clay and adobe). Wall-to-wall connections vary, with a significant portion showing strong interconnections (37.50% in Class A) and others moderate (20.83% in Class B and 37.50% in Class C). Timber diaphragms are effectively employed (83.33% in Class B), which is crucial for distributing lateral forces. Roof systems often exert lateral thrust due to stone roofing (66.67% in Class C), impacting wall stability. Despite prevalent wall openings compromising in-plane strength (70.83% in Class A), most structures (made primarily for homestay) had a higher number of openings in a lengthwise portion of the building. Consequently, the percentage of openings in such portion exceeded 25% and compromised structures' ability to withstand lateral loads. Additionally, the openings also lacked reinforcements to compensate for the reduced capacity resulting in the low-inplane index (50% in Class C and 33.33% in Class B). Further, structural heights (50% and 41.67% with multiple floors in Class C and Class B, respectively) slightly increase vulnerability to overturning. Conservation states vary, with 37.50% in acceptable condition (Class B), demanding maintenance for resilience. Moreover, none of the houses had undergone a retrofitting process and seemed to rely on cosmetic repairs. Structural irregularities in shear strength ratios (50% in Class C and 33.33% in Class B) highlight areas for improvement in seismic performance strategies tailored to local conditions. Percentage of studied buildings resembling different class for the ten parameter is shown in Figure 6.

Table 2: Wall slenderness (P1)

S. N.	Height (H)	Length (L)	Thickness (T)	Slenderness (λ)			Class
				H/T	L/T	Minimum	
1	1.22	3.01	0.45	2.70	6.68	2.70	A
2	1.25	6.00	0.45	2.78	13.33	2.78	A
3	1.40	6.38	0.45	3.10	14.18	3.10	A
4	1.37	5.75	0.45	3.05	12.77	3.05	A
5	1.48	4.81	0.45	3.28	10.68	3.28	A
6	1.78	2.61	0.45	3.95	5.80	3.95	A
7	1.50	3.96	0.45	3.33	8.80	3.33	A
8	1.61	3.26	0.45	3.58	7.25	3.58	A
9	1.58	3.84	0.3	5.26	12.79	5.26	A
10	1.44	3.24	0.45	3.21	7.20	3.21	A
11	1.87	2.58	0.45	4.15	5.74	4.15	A
12	1.40	2.28	0.45	3.12	5.06	3.12	A
13	1.60	3.66	0.45	3.55	8.14	3.55	A
14	1.55	3.88	0.45	3.43	8.62	3.43	A
15	1.29	3.12	0.45	2.87	6.93	2.87	A

S. N.	Height (H)	Length (L)	Thickness (T)	Slenderness (λ)			Class
				H/T	L/T	Minimum	
16	1.39	5.35	0.45	3.08	11.89	3.08	A
17	1.65	4.28	0.5	3.30	8.57	3.30	A
18	1.95	5.15	0.45	4.33	11.44	4.33	A
19	1.73	5.28	0.45	3.83	11.73	3.83	A
20	1.55	6.73	0.45	3.45	14.95	3.45	A
21	1.46	4.60	0.45	3.23	10.22	3.23	A
22	1.37	4.60	0.45	3.05	10.22	3.05	A
23	1.50	4.68	0.45	3.33	10.40	3.33	A
24	1.58	3.60	0.45	3.51	8.00	3.51	A

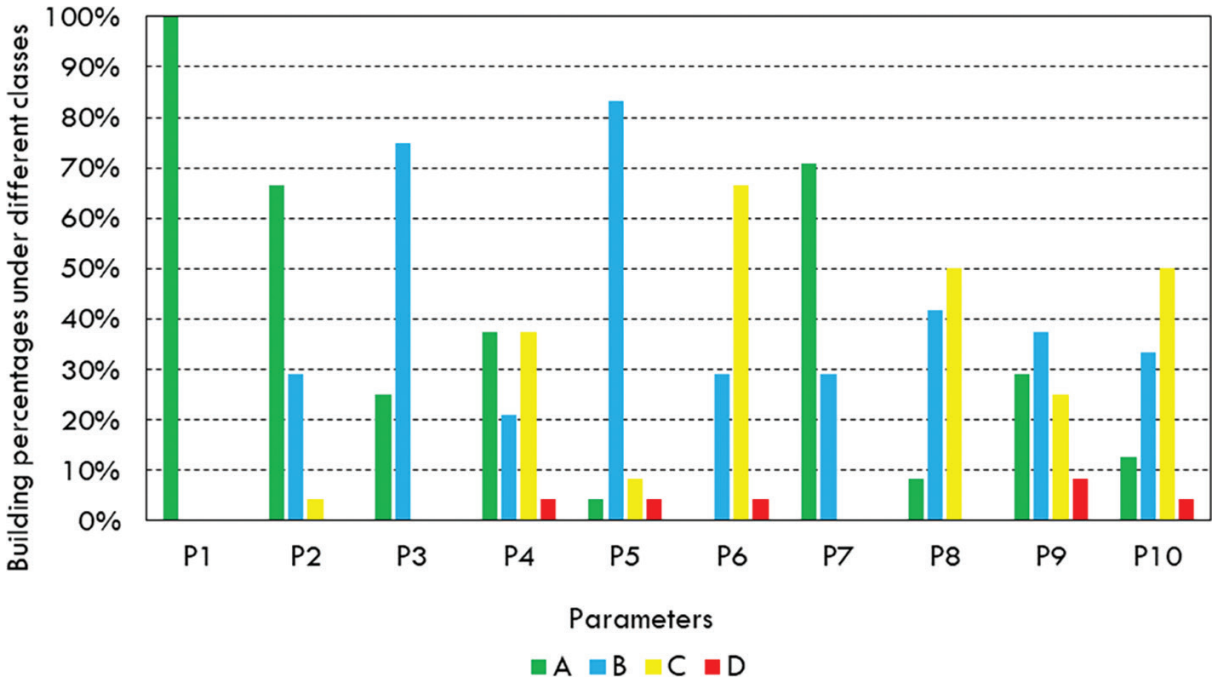

Figure 6: Percentages of buildings under different class for ten parameters

The vulnerability Index (I_v) was calculated for all 24 buildings whose values varied from 20 to 200 with a mean of 71.3 and a standard deviation of 38.95. This indicates significant variation in vulnerability levels among the buildings. Vulnerability curves were generated for all buildings using Equation (3), showing expected damage grade under earthquakes of different intensities, for the most vulnerable building (I_v = 200), the least vulnerable building (I_v = 20), and the mean value of all buildings (I_v = 71.3), as shown in Figure 7. The curve highlights priority areas for intervention, suggesting that buildings with higher I_v values require urgent mitigation measures.

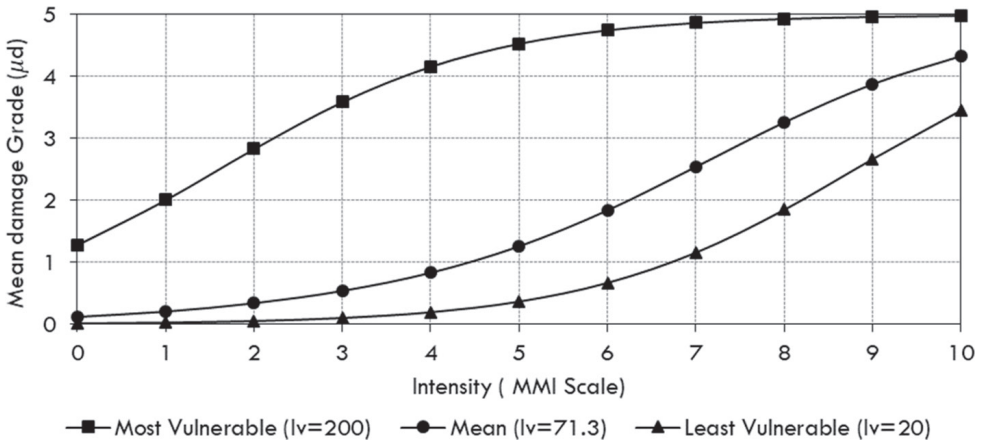

Figure 7. Vulnerability curve for the buildings in Lwang village

The vulnerability curve for the most vulnerable structure showed damage grade at zero intensity earthquake is greater than 1, primarily due to existing damage in the structure, such as roof damage and wall cracks. These existing damages are visible in Figure 8. Figure 8(a) shows the front view of the most vulnerable structure. The building seems to be in good condition from this picture. Figure 8(b) reveals the damaged roof and floor slab, with the roof precariously supported by a strut. Figure 8(c) shows the damaged roof from outside the structure. During the field investigation, numerous cracks were found in the building. Herein, one of the major cracks is shown in Figure 8(d).

(a) (b)

(c) (d)

Figure 8: Most Vulnerable Building

After plotting vulnerability curves of each building, the expected damage grades (as per EMS-98) for two earthquakes: 2023 Jajarkot earthquake (intensity VII) and 2015 Gorkha earthquake (intensity X) were determined. The expected percentage of buildings under the epicentral intensity of these two earthquakes are presented in Table 3. Results showed that during an earthquake of intensity comparable to the Jajarkot event, a significant proportion of buildings would experience moderate (37.5%) to heavy damage (45.84%). Since the intensity of 2015 Gorkha earthquake is higher i.e., X, 45.83% of the buildings are expected to suffer heavy damage and 50% could face near-collapse.

Table 3: Expected percentage of buildings to undergo different damages

Non-structural damage	Structural damage	Expected %of buildings under epicentral intensity of:	
		Jajarkot earthquake	Gorkha earthquake
Slight	None	8.33	0
Moderate	Slight	37.5	0
Heavy	Moderate	45.84	4.17
Very heavy	Heavy	0	45.83
Near collapse	Near collapse	8.33	50

The majority of the parameters were not problematic; however, parameters such as roof thrust, in-plane index, and horizontal diaphragm were areas of concern. Most buildings had slate stone roofs, which increased the seismic weight of the structures. Additionally, the dead load in the first-floor slab further increased the seismic weight. Parameters like the horizontal diaphragm and in-plane index indicated that the buildings had limited capability to resist seismic forces. The absence of other lateral load-resisting elements, such as corner stitches, rebar at corner joints, lintel bands, sill bands, gable bands, and inadequate cross walls, also contributed to the buildings' low capability in responding to seismic forces. Moreover, the majority of houses (made primarily for homestay) had a higher number of openings in a lengthwise portion of the building. Consequently, the percentage of openings in such portion exceeded 25% and compromised structures' ability to withstand lateral loads. Additionally, the openings also lacked reinforcements to compensate for the reduced capacity. Both factors, the percentage of openings and reinforcement in openings, do not satisfy the guidelines for masonry structures.

4. Conclusions

The least vulnerable building (I_v = 20) in Lwang village is constructed from brick with cement mortar, with well-executed wall-to-wall connections and steel lintel and sill bands, built after the Gorkha earthquake with no visible signs of weakening. Conversely, the most vulnerable building (I_v = 200) is made of stone with mud mortar, shows significant deficiencies in wall connections, and has severe cracks from the Gorkha earthquake. Most average houses, made of stone with mud mortar, have proper wall connections and minor cracks from the Gorkha earthquake, and feature fewer openings and cross walls, rendering them less vulnerable.

Comparing the Lwang area post-earthquake scenarios reveals significant differences in expected building damage. For the epicentral intensity in Jajarkot earthquake, the majority of buildings are anticipated to sustain moderate structural damage 45.83%, with 37.5% expected to experience slight structural damage, and a few buildings facing near-collapse damage. In contrast, for the epicentral intensity in Gorkha earthquake, 50% of buildings are expected to be near collapse, 45.83% to suffer heavy structural damage, and only a few

to have moderate structural damage.

These findings highlight the urgent need for targeted strengthening measures to enhance the seismic resilience of buildings in Lwang village, thereby safeguarding both the local community and the area's touristic value. The insights gained from this study can be applied to other regions with similar building typologies thereby contributing to mitigate the seismic vulnerability.

Acknowledgements

The authors are deeply grateful to the friends who assisted in data collection. Special thanks to the house owners of Lwang Village for their cooperation and support throughout the study.

References

Angulo-Ibáñez, Q., Mas-Tomás, Á., Galvañ-LLopis, V., & Sántolaria-Montesinos, J. L. (2012). Traditional braces of earth constructions. *Construction and Building Materials*, *30*, 389-399.

Bettinelli, P., Avouac, J.-P., Flouzat, M., Jouanne, F., Bollinger, L., Willis, P., & Chitrakar, G. R. (2006). Plate motion of India and interseismic strain in the Nepal Himalaya from GPS and DORIS measurements. *Journal of Geodesy*, *80*, 567-589.

Da Silva Vicente, R. (2009). Strategies and methodologies for urban rehabilitation interventions: vulnerability and risk assessment of the traditional building stock of the old city centre of Coimbra. University of Aveiro, Portugal.

Dolce, M., Kappos, A., Zuccaro, G., & Coburn, A. (1994). Report of the EAEE Working Group 3: Vulnerability and risk analysis. Proceedings of the 10th European Conference on Earthquake Engineering.

Ferreira, T. M., Maio, R., & Vicente, R. (2017). Seismic vulnerability assessment of the old city centre of Horta, Azores: calibration and application of a seismic vulnerability index method. *Bulletin of Earthquake Engineering*, *15*, 2879-2899.

Ferreira, T. M., Vicente, R., Mendes da Silva, J., Varum, H., & Costa, A. (2013). Seismic vulnerability assessment of historical urban centres: case study of the old city centre in Seixal, Portugal. *Bulletin of Earthquake Engineering*, *11*, 1753-1773.

Gautam, D. (2018). Observational fragility functions for residential stone masonry buildings in Nepal. *Bulletin of Earthquake Engineering*, *16*(10), 4661-4673.

Gautam, D., Adhikari, R., Rupakhety, R., & Koirala, P. (2020). An empirical method for seismic vulnerability assessment of Nepali school buildings. *Bulletin of Earthquake Engineering*, *18*(13), 5965-5982.

Gautam, D., Rupakhety, R., Adhikari, R., Shrestha, B. C., Baruwal, R., & Bhatt, L. (2021). Seismic vulnerability of Himalayan stone masonry: Regional perspectives. In *Masonry Construction in Active Seismic Regions* (pp. 25-60). Elsevier.

Khadka, B. (2020). Mud masonry houses in Nepal: A detailed study based on entire reconstruction scenario in 31 earthquake-affected districts. *Structures*.

Khakurel, S., Yeow, T. Z., Saha, S. K., & Dhakal, R. P. (2023). Post-earthquake building assessments: how long do they take? *Bulletin of the New Zealand Society for Earthquake Engineering*, *56*(2), 115-126.

Lourenço, P. B. (1996). A user/programmer guide for the micro-modeling of masonry structures. *Report*, *3*(1.31), 35.

Lourenço, P. B., Oliveira, D. V., Leite, J. C., Ingham, J., Modena, C., & da Porto, F. (2013). Simplified indexes for the seismic assessment of masonry buildings: International database and validation. *Engineering Failure Analysis*, *34*, 585-605.

Masciotta, M.-G., Ramos, L. F., Lourenço, P. B., & Matos, J. A. (2016). Development of key performance indicators for the structural assessment of heritage buildings. 8th European Workshop on Structural Health Monitoring, EWSHM.

Mendes, N., & Lourenço, P. B. (2015). Seismic vulnerability of existing masonry buildings: Nonlinear parametric analysis. *Seismic Assessment, Behavior and Retrofit of Heritage Buildings and Monuments*, 139-164.

Neves, F., Costa, A., Vicente, R., Oliveira, C. S., & Varum, H. (2012). Seismic vulnerability assessment and characterisation of the buildings on Faial Island, Azores. *Bulletin of Earthquake Engineering*, *10*, 27-44.

NHPC. (2021). National Housing Population Census. Kathmandu: National Statistics Office.

Ortega, J., Vasconcelos, G., Rodrigues, H., & Correia, M. (2018). Assessment of the influence of horizontal diaphragms on the seismic performance of vernacular buildings. *Bulletin of Earthquake Engineering*, *16*, 3871-3904.

Ortega, J., Vasconcelos, G., Rodrigues, H., & Correia, M. (2019). A vulnerability index formulation for the seismic vulnerability assessment of vernacular architecture. *Engineering Structures*, *197*, 109381.

Shakya, M., Varum, H., Vicente, R., & Costa, A. (2014). A new methodology for vulnerability assessment of slender masonry structures. Proceedings of the 2nd European conference on earthquake engineering & seismology.

Spence, R., & D'Ayala, D. (1999). Damage assessment and analysis of the 1997 Umbria-Marche earthquakes. *Structural Engineering International*, *9*(3), 229-233.

Upadhyay, M., Budhathoki, P., Dhakal, N., Tiwari, L., Pun, S., Barma, R., & Khakurel, S. (2024). Seismic Vulnerability Assessment of Historic Masonry Structure: A Case Study of Bindhyabasini Temple. 15th IOE Graduate Conference.

Upreti, B. (1999). An overview of the stratigraphy and tectonics of the Nepal Himalaya. *Journal of Asian Earth Sciences*, *17*(5-6), 577-606.

Vicente, R., Parodi, S., Lagomarsino, S., Varum, H., & Silva, J. M. (2011). Seismic vulnerability and risk assessment: case study of the historic city centre of Coimbra, Portugal. *Bulletin of Earthquake Engineering*, 9, 1067-1096.